Steric Effect in Electron−Molecule Interaction

Yigal Lilach and Micha Asscher*

Department of Physical Chemistry and The Farkas Center for Light Induced Processes, The Hebrew University, Jerusalem 91904, Israel

Received: October 21, 2003

A steric effect has been identified and measured in the interaction of electrons with oriented molecules, for the first time. Photoelectron mediated reactivity has been determined, with a cross section of $\sigma = (3.0 \pm 0.4) \times 10^{-19}$ cm^2 (methyl down) for an adsorbed CD_3Br on O/Ru(001). A three times smaller cross section was obtained for the bromine down configuration, controlled by oxygen precoverage. A qualitatively similar molecular orientation dependent effect was measured by direct bombardment with 10 eV electrons, however, at much larger cross sections. The significance of the steric effect reported here for electron-transfer processes in general is discussed.

Introduction

Steric effects are among the oldest and most intuitive concepts in chemical reactivity. Chemists have recognized very early that proper mutual orientation of reactants is almost as important as energetic requirements for a successful reactive encounter. One experimental approach to study molecular orientation dependent reactivity has been via molecular beam studies in the gas phase, a focus of interest two decades ago. In these studies, electrostatic hexapole technology has been employed to orient molecules in a beam and then collide them with alkali metals[1−4] and other electron-donating atoms.[5]

For many years the multiple and diverse aspects of electron−molecule interactions have been at the focus of basic science research in both chemistry and biology. Studies in this field have included inter- and intramolecular electron transfer,[6] transmission[7−9] conduction within and through molecules,[10,11] and dissociative electron attachment (DEA) processes.[12−14] Recent interest in molecular electronics has brought the basic science in this field closer to modern technology than ever before.[8−11]

Here we present, for the first time, the phenomenon of molecular orientation dependent electron−molecule interaction. Specifically, by tuning of the oxygen coverage on ruthenium, the orientation of methyl bromide could be controlled bromine down or methyl down on O/Ru(001). Similar behavior was reported in the coadsorption system of potassium with water on Pt(111).[15,16]

UV irradiation at a photon energy of 6.4 eV revealed enhanced reactivity of substrate-mediated DEA and electron-stimulated desorption (ESD) of the methyl down orientation by a factor of 3. Similar sensitivity to the molecular orientation, although with a smaller effect, was measured by low-energy electrons directly bombarding the oriented adsorbates, approaching the molecules from the opposite direction, namely the vacuum side.

Experimental Section

The photochemistry experiments described below were performed in an ultrahigh vacuum (UHV) apparatus, described elsewhere in detail.[17] It is equipped with LEED/Auger, a quadrupole mass spectrometer (QMS) for temperature-programmed desorption (TPD) and for real time detection of desorbing molecules during laser irradiation and electron bombardment. Adsorbates orientation could be determined by means of a Kelvin probe, operated in a differential $\Delta\varphi$-TPD mode as explained elsewhere in detail.[17,18] A mini excimer laser was operated at 193 nm, 1 mJ/pulse, at variable repetition rate up to 100 Hz. Low-energy electrons at 10 eV kinetic energy bombarded the adsorbate system via a retarding grid that decreased the electrons energy from 100 eV at a typical sample current of 0.1 μA. The Ru(001) sample, oriented to within 0.1 deg of the (001) plane, could be cooled to 82 K by pumping over a liquid-nitrogen reservoir attached to the sample and heated to 1650 K for annealing, with temperature stabilized to 0.5 deg or ramping of its temperature via resistive heating ac coupled routine. The temperature was monitored by means of a W5Re/W26Re thermocouple.

Results and Discussion

Methyl bromide thermally dissociates on a clean Ru(001) at coverages below 0.2 ML.[19] Adsorbing 0.25 ML of oxygen on Ru(001) and annealing to 400 K results in an ordered (2×2)O−Ru(001) structure.[20,21] This oxygen coverage suffices to completely passivate the ruthenium surface against dissociation of CD_3Br, as indicated by the absence of any D_2 signal in ΔP-TPD (not shown) following CD_3Br adsorption on that surface at 82 K. Gradually increasing the annealed oxygen precoverage above 0.25 ML and then covering it by 1.5 ML of CD_3Br results in the ΔP-TPD and differential $(d(\Delta\phi)/dT)$ $\Delta\Phi$-TPD spectra shown in Figure 1. There are three distinct peaks in ΔP-TPD, denoted β_1, β_2, and α. The relatively high temperature of the β_1 peak and its width are associated with binding energy (E_b) of 17.8 kcal/mol (resulting from full TPD line shape analysis) of CD_3Br molecules to O/Ru and a significant repulsive interaction among the adsorbates. The $d(\Delta\phi)/dT$ spectrum indicates (positive change) that all the β_1 molecules adsorb with their bromine end down toward the surface. The α peak at 120 K is due to molecules desorbing from the second layer (E_b = 7.7 kcal/mol). As previously discussed in detail,[19] the second layer of CD_3Br on the clean Ru(001) is adsorbed with its methyl

* To whom correspondence should be addressed. E-mail: asscher@fh.huji.ac.il.

10.1021/jp031177t CCC: $27.50
Published on Web 03/16/2004

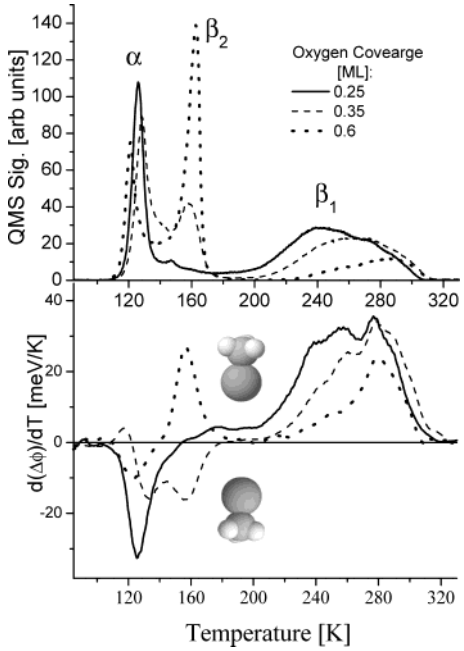

Figure 1. Δ*P*-TPD (top) and ΔΦ-TPD (bottom) of 1.5 ML CD_3Br on several oxygen precoverages. The heating rate was 2 K/s.

end down (negative change in the d($\Delta\phi$)/dT spectrum). Increasing the oxygen coverage above 0.25 ML introduces a new adsorption site (β_2). These molecules desorb at 160 K (E_b = 9.6 kcal/mol).

The total desorption peak area ($\alpha + \beta_1 + \beta_2$ sites) of the methyl bromide Δ*P*-TPD spectra is invariant with oxygen precoverage to within 5% of our experimental uncertainty, indicating that the sticking probability of CD_3Br is insensitive to the oxygen coverage. The appearance of the β_2 molecules suggests that as the oxygen precoverage increases, CD_3Br molecules are displaced from the β_1 adsorption sites into the β_2 sites.

The interesting observation in Figure 1 is that the *orientation* of the β_2 molecules is sensitive to the local surface density of adsorbed oxygen. This is inferred from the opposite sign of the relevant d($\Delta\phi$)/dT peak at 160 K (Figure 1). This is a justified interpretation of the work function change spectrum as long as no molecular dissociation takes place. In fact, work function change measurements in the differential mode are expected to be more sensitive and relevant for the determination of overall molecular orientation with respect to the surface than, e.g., IR measurements. At oxygen coverage of 0.35 ML the β_2 molecules are arranged with their methyl down, while at 0.6 ML of oxygen they switch to the bromine down configuration.

Once the ability to control molecular orientation has been confirmed it becomes an ideal model system to examine the sensitivity of electron−molecule interaction to molecular orientation by employing substrate-mediated photoelectrons and direct electron-induced desorption and dissociation.

Differential ΔΦ-TPD spectra following 6.4 eV photons irradiation of 0.8 ML CD_3Br adsorbed on 0.6 ML O/Ru are shown in Figure 2A, for different irradiation times. The excimer laser power density at the sample was about 1 MW/cm^2, or 2.4×10^{16} photons/s. The same experiments were performed at 0.35 ML oxygen, Figure 2B. Both the β_1 and β_2 molecules undergo photodesorption and photofragmentation, which lead to an exponential decay of the relevant differential ΔΦ-TPD peak intensity. A plot of the logarithm of the integrated area under the d($\Delta\phi$)/dT spectra for both peaks vs the number of

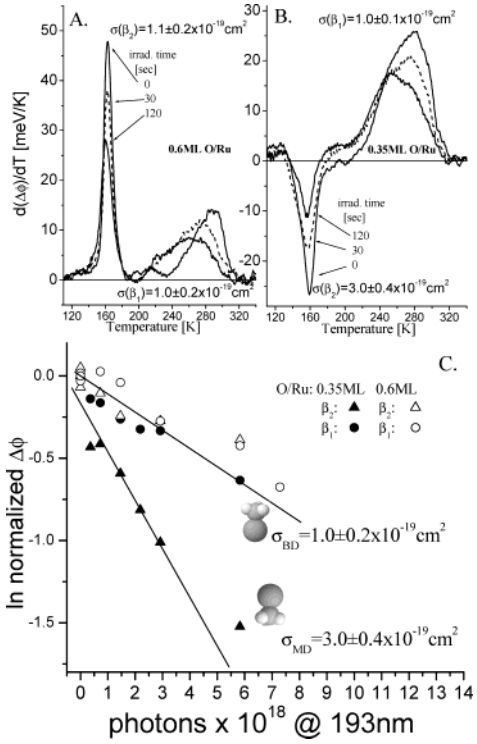

Figure 2. ΔΦ-TPD of 0.8 ML of CD_3Br adsorbed on 0.6 ML O/Ru(001) (A) and 0.35 ML O/Ru(001) (B), following the indicated irradiation times by 193 nm UV laser irradiation. The photons flux was 2.4×10^{16} photons/s at the sample surface. (C) Cross section determination for depletion of the β_1 and β_2 differential work function change peaks shown in (A) and (B).

photons should result in a linear plot. The initial slope of such plots determines the cross section for the photoreaction. In Figure 2C such plots are presented.

The cross sections obtained this way can clearly be separated into two groups: the removal of the β_1 molecules (bromine down = BD) in both oxygen coverages and that of the β_2 molecules on top of 0.6 ML O/Ru is at a cross section $\sigma_{BD} = (1.0 \pm 0.2) \times 10^{-19}$ cm^2. In contrast, the β_2 molecules that reside on top of 0.35 ML O/Ru, *and are oriented methyl down* (MD), are removed at $\sigma_{MD} = (3.0 \pm 0.4) \times 10^{-19}$ cm^2.

We find that molecules adsorbed at the same orientation (BD) but at different binding sites at different adsorption energies (β_1 and β_2 over 0.6 ML O/Ru) possess the same overall removal (desorption + dissociation) cross section. At the same time, the more weakly bound molecules that are flipped to the MD configuration are removed at a cross section that is three times larger. It is interesting to note that despite the different electronic configurations of the surface dictated by different oxygen coverage, the molecular orientations MD and BD within the β_2 sites are bound at exactly the same energy to the surface, as indicated by the TPD data in Figure 1. This, we believe, emphasizes the dominance of the molecular *orientation* in determining the cross section for the electron−molecule interaction.

Orientation-dependent electron−molecule interaction could be detected also by following the real-time desorption of CD_3Br molecules during the UV irradiation. The QMS signal at mass 97 during continuous exposure to photons is shown in Figure 3 (left frames), for the oxygen and CD_3Br coverages discussed above. The cross section is extracted from the expression $I(t) = I(0)e^{-\sigma Ft}$, where $I(t)$ is the QMS signal, F is the photons flux in photons/cm^2, and σ is the photoelectron-mediated desorption cross section in cm^2. As before, only the

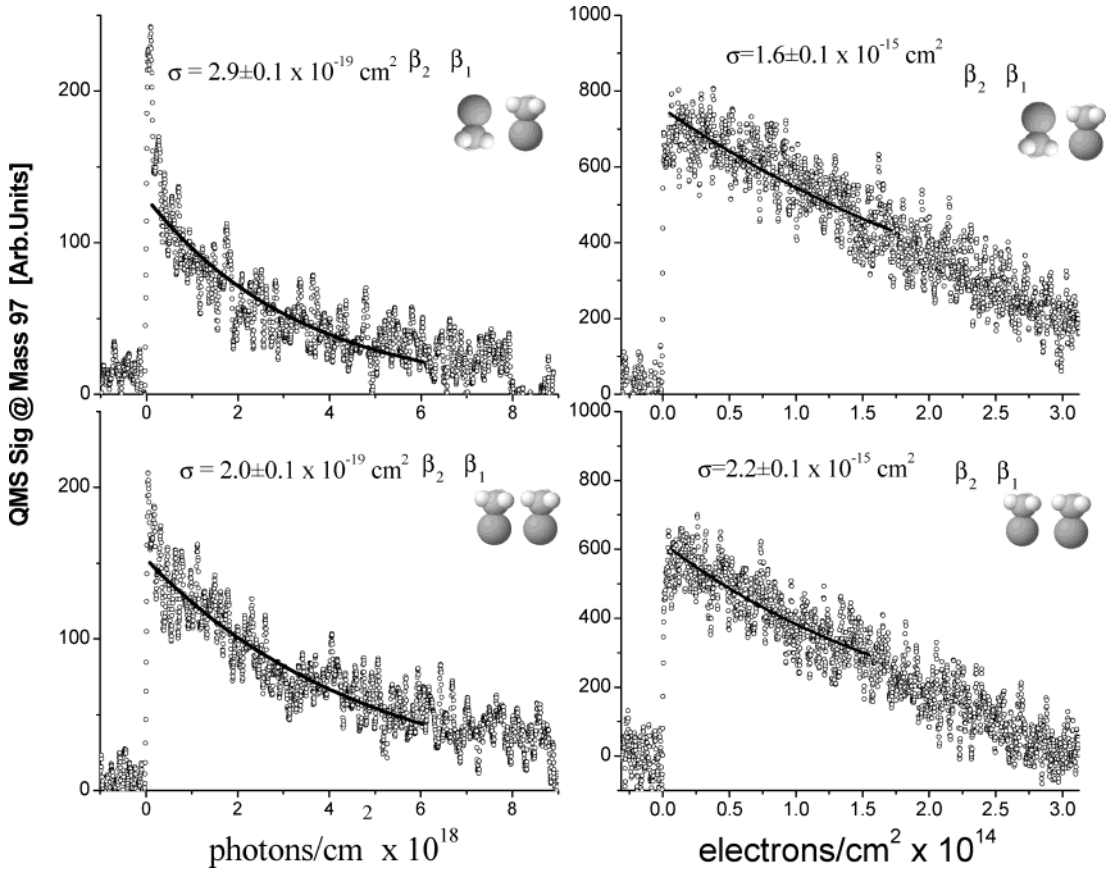

Figure 3. QMS signal at mass 97 (open circles) during irradiation of 0.8 ML CD_3Br on 0.35 ML O/Ru(001) (top) and 0.6 ML O/Ru(001) (bottom). Irradiation consisted of photoelectrons generated from 193 nm photons (left panels) and direct 10 eV electrons from the gas phase (right panels). The initial decay was fitted to an exponent (solid line) to extract the cross section for desorption.

initial 6×10^{18} photons are considered. This is important to minimize the influence of photofragments on the tail of the decay curve. The measured cross sections are $\sigma_{BD} = (2.0 \pm 0.1) \times 10^{-19}$ cm^2 and $\sigma_{MD} = (2.9 \pm 0.1) \times 10^{-19}$ cm^2 for the 0.6 ML O/Ru (BD) and 0.35 ML O/Ru (MD), respectively.

The QMS signal includes photodesorption from both β_1 and β_2 sites, but it is insensitive to photofragmentation (DEA). The identical cross section obtained by the real-time QMS detection and the work function change measurements is explained assuming that photoelectron-mediated *desorption* is the dominant process in the MD configuration (0.35 ML O/Ru). Dominance of the electron-mediated *dissociative* channel in the MD configuration of the β_2 molecules would have resulted in smaller integrated differential work function change near 160 K. This is due to the negative work function change contribution of the two dissociation fragments, methyl and bromine,[19,22] if they separately adsorb on the surface. If fragments (e.g. methyl) are ejected to the gas phase, the overall work function change and thus the measured cross section are again expected to be similar to the electron-mediated parent molecular desorption. A total of 15 ± 5% of the parent molecules dissociate, and their methyl fragments stay on the surface and further dissociate. This is established by the postirradiation TPD of D_2, obtained due to several consecutive photogenerated dissociation events of methyl and smaller fragments on the surface.[23,24]

Real-time desorption was measured also for irradiation with 10 eV electrons, as seen in Figure 3 (right frames). The cross sections for direct electron-stimulated desorption are 4 orders of magnitude larger than those for the photoelectron-mediated desorption. Observations of similar nature were previously reported for a related system.[25] A steric effect has been measured also in the case of the direct ESD, although a smaller magnitude was detected. As expected, however, the difference between the two orientations has the opposite trend, namely the removal cross section of MD molecules is *smaller* than that of the BD molecules. As in the photoelectron-mediated case discussed above, also here the difference in the cross section is attributed to steric effect in electron−molecule collision, where the reaction $CD_3Br + e^-$ has a larger cross section when the electron approaches the molecule from the methyl end.

One should consider alternative mechanisms to explain the enhanced probability for both photoinduced and electron-induced desorption of methyl bromide from the O/Ru(001) surface when the methyl faces the direction of approach of the electrons. One such explanation is the enhanced quenching rate at the bromine down (BD) configuration. Such a mechanism may be justified if we consider that most of the negative charge resides on the bromine side of the molecule following electron attachment. In this case, the larger charge density on the bromine side should overlap higher electron density of the metal when the bromine faces the surface since it is closer to the surface than when it is in the methyl down (MD) configuration. Larger charge density overlap often results in shorter excited-state lifetime or faster quenching back to the ground state. Shorter lifetime results, therefore, in a smaller probability for electron-induced desorption, as preliminary wave packet dynamical simulations indicate.[26] While this argument qualitatively explains the steric effect found in the photoinduced substrate-mediated desorption of methyl bromide at photon energy of 6.4 eV, it cannot simultaneously rationalize the opposite steric effect found in the enhanced electron-stimulated desorption data.

Conclusions

We conclude that the steric effect has indeed been identified and measured, for the first time, within the initial attachment step of the interaction of collimated electrons with preoriented molecules. Control over the molecular orientation of adsorbed CD_3Br was achieved by varying oxygen precoverage on Ru(001). When a flux of photoelectrons generated at the bulk metal strikes adsorbed methyl bromide from the methyl end, the overall electron mediated reactivity has a cross section of $\sigma = 3.0 \times 10^{-19}$ cm^2, which is three times larger than the cross section determined for the bromine down configuration. Qualitatively similar results were obtained by direct bombardment with 10 eV electrons from the gas phase but at cross sections that are 4 orders of magnitude larger.

The steric effect reported here is central for our basic understanding of electron-transfer processes, among the most fundamental concepts in chemical reactivity.[27] Photosynthesis is an example of a biological system that functions via a cascade of electron-transfer processes. Only in recent years the detailed mutual structure of the complex molecular elements of photosystem-I has been scrutinized by means of X-ray diffraction analysis of the relevant proteins.[28] Steric effects in such complex systems, if studied, may reveal some of the mysterious driving forces that lead to a naturally chosen structure over the others.

Acknowledgment. This work was partially supported by a grant from the U.S.−Israel Binational Foundation and the Israel Science Foundation. The Farkas center is supported by the Bundesministerium fur Forschung und Technologie and the Minerva Gesellschaft fur die Forschung mbh.

References and Notes

(1) Brooks, P. R. *Science* **1976**, *193*, 11.
(2) Parker, D. H.; Bernstein, R. B. *Annu. Rev. Chem. Phys*. **1989**, *40*, 561.
(3) Bernstein, R. B.; Herschbach, D. R.; Levine, R. D. *J. Phys. Chem*. **1987**, *91*, 5365.
(4) Parker, D. H.; Jalink, H.; Stolte, S. *J. Phys. Chem*. **1987**, *91*, 5427.
(5) Janssen, M. H.; Parker, D. H.; Stolte, S. *J. Phys. Chem*. **1991**, *95*, 8142.
(6) Marcus, R. A. *J. Chem. Phys*. **1965**, *43*, 679.
(7) Caron, L. G.; Perluzzo, G.; Bader, G.; Sanche, L. *Phys. Rev*. **1985**, *B33*, 3027.
(8) Naaman, R.; Haran, A.; Nitzan, A.; Evans, D.; Galperin, M. *J. Phys. Chem*. **1998**, *102* (19), 3658.
(9) Ray, R.; Ananthavel, S. P.; Waldeck, D. H.; Naaman, R. *Science* **1999**, *283*, 814.
(10) (a) Reed, M. A.; Zhou, C.; Muller, C. J.; Burgin T. P.; Tour, J. M. *Science* **1997**, *278*, 252. (b) Segal, D.; Nitzan, A.; Davis, W. B.; Wasilewski, M. R.; Ratner, M. A. *J. Phys. Chem*. **2000**, *B104*, 3817. (c) Nitzan, A. *J. Phys. Chem*. **2001**, *A105*, 2677.
(11) Porath, D.; Bezryadin, A.; de Vries, S.; Dekker, C. *Nature* **2000**, *403*, 635.
(12) Sanche, L. *Scanning Microsc*. **1995**, *9*, 619.
(13) Negesha, K.; Fabrikant, I. I.; Sanche, L. *J. Chem. Phys*. **2001**, *114* (11), 4934.
(14) Burrow, P. D.; Aflatooni, K. *J. Chem. Phys*. **2002**, *116* (13), 5471.
(15) Bonzel, H. P.; Pirug, G.; Muller, J. E. *Phys. Rev. Lett*. **1987**, *58*, 2138.
(16) Muller, J. E. In *Physics and Chemistry of Alkali Metals Adsorption*; Bonzel, H. P., Bradshaw, A. M., Ertl, G., Eds.; Elsevier: Amsterdam, 1989; p 271.
(17) Livneh, T.; Lilach, Y.; Asscher, M. *J. Chem. Phys*. **1999**, *111* (24), 11138.
(18) Lilach, Y.; Asscher, M. *J. Chem. Phys*. **2002**, *117*, 6730.
(19) Livneh, T.; Asscher, M. *J. Phys. Chem*. **1997**, *B101*, 7505.
(20) Lindroos, M.; Pfnur, H.; Held, G.; Menzel, D. *Surf. Sci*. **1989**, *222*, 451.
(21) Gsell, M.; Stichler, M.; Jakob, P.; Menzel, D. *Isr. J. Chem*. **1998**, *38*, 339.
(22) Livneh, T.; Asscher, M. *J. Phys. Chem*. **2003**, *B107*, xxxx.
(23) Kis, A.; Kiss, J.; Solymosi, F. *Surf. Sci*. **2000**, *459*, 149.
(24) Lilach, Y. Ph.D. Thesis, Hebrew University, 2003.
(25) Junker, H. H.; White, J. M. *Surf. Sci*. **1997**, *382*, 67.
(26) Jorgensen, S.; Zeiri, Y.; Asscher, M.; lilach Y.; Kosloff, R. Manuscript in preparation.
(27) (a) Kuznetsov, A. M. *Charge Transfer in Physics, Chemistry and Biology*; Gordon & Breach: New York, 1995. (b) In *Electron Transfer-From Isolated Molecules to Biomolecules*; Jortner, J., Bixon, M., Eds.; Wiley: New York, 1999; Vol. 106.
(28) (a) Krau, N.; Hinrichs, W.; Witt, I.; Fromme, P.; Pritzkow, W.; Dauter, Z.; Betzel, C.; Wilson, K. S.; Witt, H. T.; Saenger, W. *Nature* **1993**, *361*, 326. (b) Krau, N.; Schubert, W.-D.; Klukas, O.; Fromme, P.; Witt, H. T.; Saenger, W. *Nat. Struct. Biol*. **1996**, *3*, 965.